



UNIVERSIDADE ESTADUAL DE CAMPINAS
SISTEMA DE BIBLIOTECAS DA UNICAMP
REPOSITÓRIO DA PRODUÇÃO CIENTÍFICA E INTELLECTUAL DA UNICAMP

Versão do arquivo anexado / Version of attached file:

Versão do Editor / Published Version

Mais informações no site da editora / Further information on publisher's website:

<https://academic.oup.com/jb/article/170/1/51/6143041#303917160>

DOI: 10.1093/jb/mvab020

Direitos autorais / Publisher's copyright statement:

©2021 by Oxford University Press. All rights reserved.

DIRETORIA DE TRATAMENTO DA INFORMAÇÃO

Cidade Universitária Zeferino Vaz Barão Geraldo

CEP 13083-970 – Campinas SP

Fone: (19) 3521-6493

<http://www.repositorio.unicamp.br>

Components from spider venom activate macrophages against glioblastoma cells: new potential adjuvants for anticancer immunotherapy

Received December 10, 2020; accepted February 13, 2021; published online February 18, 2021

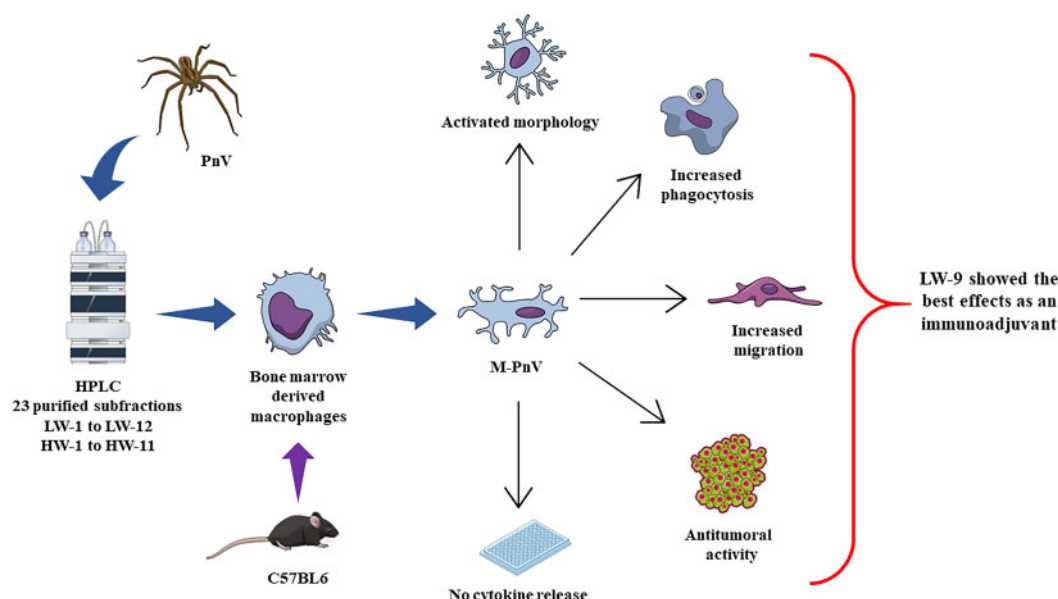
Jaqueline Munhoz ¹, Gabriela Peron²,
Amanda Pires Bonfanti^{1,2}, Janine Oliveira²,
Thomaz A. A. da Rocha-e-Silva³,
Rafael Sutti⁴, Rodolfo Thomé^{2,5},
André Luís Bombeiro², Natalia Barreto^{1,2},
Ghanbar Mahmoodi Chalbatani⁶,
Elahe Gharagouzloo⁷,
João Luiz Vitorino-Araujo⁸, Liana Verinaud²
and Catarina Rapôso^{1,*}

*Catarina Rapôso, Faculty of Pharmaceutical Sciences, State University of Campinas (UNICAMP), Cândido Portinari, 200 - Cidade Universitária, Campinas, São Paulo, 13083-871, Brazil. Tel.: +55-19-983798091, email: raposo@unicamp.br

¹Faculdade de Ciências Farmacêuticas, Universidade Estadual de Campinas (UNICAMP). Cândido Portinari, 200 - Cidade Universitária, Campinas, São Paulo, 13083-871, Brazil; ²Departamento de Biologia Estrutural e Funcional, Instituto de Biologia, UNICAMP. Av. Bertrand Russel, Campinas, São Paulo, 13083-865, Brazil; ³Faculdade Israelita de Ciências da Saúde Albert Einstein, São Paulo, SP, 05652-900, Brazil; ⁴Faculdade de Ciências Médicas, Santa Casa de São Paulo. Dr. Cesário Motta Jr., 61, Vila Buarque, São Paulo, SP, 01221-020, Brazil; ⁵Department of Neurology, Thomas Jefferson University, 909 Walnut St #3, Philadelphia, PA, 19107, USA; ⁶Department of Immunology and Biology, TUMS School of Medicine, Poursina Road, Tehran, 1417613151, Iran; ⁷Cancer Institute, Keshavarz Blvd, Tehran University of Medical Science, Tehran, 1419733141, Iran; and ⁸Disciplina de Neurocirurgia, Faculdade de Ciências Médicas da Santa Casa de São Paulo. Dona Veridiana, 56 - Higienópolis, São Paulo - SP, 01238-010, Brazil

Immunomodulation has been considered an important approach in the treatment of malignant tumours. However, the modulation of innate immune cells remains an under-explored tool. Studies from our group demonstrated that the *Phoneutria nigriventer* spider venom (PnV) administration increased the infiltration of macrophage in glioblastoma, in addition to decreasing the tumour size in a preclinical model. The hypothesis that PnV would be modulating the innate immune system led us to the main objective of the present study: to elucidate the effects of PnV and its purified fractions on cultured macrophages. Results showed that PnV and the three fractions activated macrophages differentiated from bone marrow precursors. Further purification generated 23 subfractions named low weight (LW-1 to LW-12) and high weight (HW-1 to HW-11). LW-9 presented the best immunomodulatory effect. Treated cells were more phagocytic, migrated more, showed an activated morphological profile and induced an increased cytotoxic effect of macrophages on tumour cells. However, while M1-controls (LPS) increased IL-10, TNF-alpha and IL-6 release,

Graphical Abstract



Phoneutria nigriventer spider venom (PnV) modulates bone marrow-derived macrophages in a activate profile with antitumoural activity in glioblastoma cells. Furthermore, the screening showed that LW-9 presented the best immunomodulatory effect. Treated cells were more phagocytic, migrated more, showed an activated morphological profile and induced an increased cytotoxic effect of macrophages on tumour cells and did not alter any cytokine, with the exception of LW-9 that stimulated IL-10 production. These findings suggest that molecules present in LW-9 have the potential to be used as immunoadjuvants in the treatment of cancer.

PnV, fractions and subfractions did not alter any cytokine, with the exception of LW-9 that stimulated IL-10 production. These findings suggest that molecules present in LW-9 have the potential to be used as immunoadjuvants in the treatment of cancer.

Keywords: glioma; immunomodulation; innate immune system; phagocytosis; *Phoneutria nigriventer*.

Abbreviations: BHI, Brain Heart Infusion; CAR-T, chimeric antigen receptor T-cell; CFU, colony forming units; ELISA, enzyme-linked immunosorbent assay; FBS, foetal bovine serum; HPLC, high-pressure liquid chromatography; HW, high weight; IMDM, Iscove's Modified Dulbecco's Media; LILRB1, leukocyte immunoglobulin-like receptor B1; LW, low weight; LPS, lipopolysaccharide; PBS, phosphate-buffered saline; PD-1, programmed cell death 1; TAMs, tumour-associated macrophages; TCR-T, T-cell receptor-engineered T-cell; TFA, trifluoroacetic acid; TME, tumour microenvironment.

Immunotherapy against cancer has been considered as a fundamental and important pillar to improve the prognosis of malignancies. This therapy uses the abilities of the immune system components, including cytokines, antibodies and cells, to recognize and eliminate malignant cells (1). The first antibody therapy was approved by the FDA in the late 1990s for cancer treatment, to be used alone or in combination with surgery, chemotherapy and radiation (2–5). Strategies targeting the adaptive immune system, such as specific antibodies against T lymphocyte-associated antigen 4 (CTLA-4) or against programmed cell death 1 (PD-1) and its ligand PD-L1, were the first approved therapies. Adoptive cell therapies, such as with TCR-T (T-cell receptor-engineered T-cell) and CAR-T (chimeric antigen receptor T-cell), are also an approved approach (6, 7). These are now as the first line of therapy for some types of cancer, such as melanoma, non-small cell lung cancer and Hodgkin's lymphoma (3, 8, 9). However, such strategies can induce resistance and there is evidence of severe adverse effects (3, 9–11).

Drugs that act on myeloid and lymphoid cells of the innate immune system, *e.g.* natural killer cells and macrophages, or that can act on both innate and adaptive systems, have recently emerged as relevant therapies in many types of solid tumours and haematopoietic cancers (3, 9). It has already been described that modulating macrophages may be a more promising strategy compared to try killing tumour cells, because macrophages kill malignant cells, reorganize the extracellular matrix, recycle debris originated from cells and molecules, start signalling to cell growth and stimulate the migration of cells to repair the tissue (12). However, modulating macrophages as a strategy to treat cancer is an underexplored field.

Macrophages are sentinel cells of the innate immune system and multifunctional antigen-presenting cells (13, 14). They have the ability of engulf and brake down pathogens, toxins, cellular debris among other targets, providing the first line of immune defense. These properties make macrophages promising cells for the treatment of malignant tumours, mainly because they can also activate the entire immune system against foreign and diseased cells (15). Macrophages exist in a diverse collection of cell types and, under different external stimuli, can oscillate between different activation profiles (16, 17). These macrophages are classically referred to as activated (M1—proinflammatory) or alternatively activated (M2—antiinflammatory), and although this simple concept of M1/M2 can explain the phenotypic heterogeneity of these cells, in fact, macrophages appear to exist in different populations with an extensive variety of polarization states (13).

Macrophages infiltrate the malignant tumour microenvironment (TME) in large numbers, being called tumour-associated macrophages (TAMs). Many studies in the last decade have revealed that TAMs play a protumour role and are related to the cancer progression (13, 18). However, the role of macrophages in cancer has been described as complex and paradoxical (19). Usually, they are considered synonymous of M2-macrophages, but studies have shown that TAMs are a group of macrophages with transcriptional and phenotypic characteristics distinct from the M1 and M2 subsets (10). The main strategies to use TAMs as targets for immunotherapy are related to: (1) reeducating macrophages, from a protumour profile, generally described as M2, to an antitumour profile, characterized as M1-like cell; (2) blocking the recruitment or survival of macrophages in the tumour; (3) promoting the activation of macrophage and (4) using monoclonal antibodies or molecules that increase the killing activity and/or phagocytosis functions, promoting the destruction of cancer cells (17, 20, 21).

Since the first demonstration of cytoskeletal impairment in astrocytes treated with the venom of the South American wandering spider *Phoneutria nigriventer* (PnV) (22), a sequence of studies by our group exhibited the effects of PnV on glioblastoma (GB) cell lines *in vitro* and *in vivo*. The venom has cytotoxic and antimigratory effects, arrested the cell cycle in G0 and reduced or eradicated tumour development in a xenogeneic model, in addition to increasing the infiltration of macrophages in the TME (23–25). Those previous findings led us to herein investigate the modulatory effect of PnV and its components on macrophages, and to find out whether and which of those molecules have the potential to act as immunoadjuvant in cancer treatment.

Methodology

Reagents and venom

The reagents were purchased from Sigma–Aldrich (St. Louis, MO), unless otherwise specified. *Phoneutria*

nigriventer venom samples were extracted from several adult spiders by electrical stimulation. The pattern of the crude venom was analysed by high-pressure liquid chromatography (HPLC) and compared with other samples used and published. The fractionation of the venom was done by Amicon Ultra Centrifugal Filter (#UFC801008; Thermo Fisher Scientific, Suwanee, GA), following Santos *et al.* (23). With this procedure, PnV was fractionated by molecular mass, resulting in three fractions: F1 = <3 kDa; F2 = between 3 and 10 kDa and F3 = above 10 kDa. Venom and fractions were lyophilized and stored at -80°C . The three fractions were used in experiments conducted to select the most significant among them, considering the macrophages modulation. After this first screening, F1 and F2 together were called low weight (LW) components, while F3 alone was named high weight (HW) components. LW and HW were purified again by reversed phase HPLC, using a Shimadzu VP-ODS column, 0.1% trifluoroacetic acid (TFA) as mobile phase and 90% acetonitrile 0.1% TFA as eluent. Twelve purified components were obtained from LW, named subfractions LW-1–LW-12, and 11 from HW, named subfractions HW-1–HW-11.

Cell cultures and treatments

Bone marrow-derived macrophages Murine bone marrow cells were cultured with the supernatant of fibroblasts (L929) cell line for differentiation in macrophages. All experiments were conducted in accordance with the Ethical Principles on Animal Research, adopted by the Brazilian College on Animal Experimentation (Colégio Brasileiro de Experimentação Animal—COBEA), with the prior approval of the Ethics Committee on the Use of Animals (CEUA) of the Universidade Estadual de Campinas (UNICAMP) (#5118-1/2019). Male C57BL6 mice at 7–10 weeks of age were euthanized by overdosage of the association of dissociative anaesthetic (ketamine, 300 mg/kg) and alpha 2 adrenoreceptor agonist (xylazine, 30 mg/kg) administered intraperitoneally, and bone marrow precursors were collected from femurs. Briefly, immediately after collecting from marrow, the cell suspension was cultivated in Petri dishes with 10 ml IMDM (Iscove's Modified Dulbecco's Media) supplemented with 20% foetal bovine serum (FBS) and 30% L929 cell supernatant (as a source of macrophage colony-stimulating factor). After 4 days, more 10 ml of fresh medium with the same proportions was added (26). After incubation of this culture for 7 days at 37°C and 5% of CO_2 , the cells were washed with phosphate-buffered saline (PBS) and the adherent cells were reaped with a cell scraper for use in different assays, as described below.

Human glioblastoma cell line (NG97) Human glioblastoma (NG97) cells were donated by a patient from the Hospital das Clínicas/Universidade Estadual de Campinas (HC/UNICAMP) and the cell line was established and characterized in a sequence of published studies (27–31). The culture was maintained in IMDM supplied with 10% FBS, 100 U/ml penicillin and 100 $\mu\text{g}/\text{ml}$ streptomycin, at 37°C and 5% of CO_2 .

After four passages from the defrosting, cells were seeded at a density of 1×10^4 per cm^2 in a 25 cm^2 culture bottle and grown in IMDM containing 10% FBS and 100 UI/ml penicillin and streptomycin (pH 7.4) (Gibco). After confluence, the cells were detached using a scraper and placed in 48-well plates.

Treatments After differentiation, the macrophages were preactivated with 20 ng/ml of recombinant mouse IFN- γ (BD #554587) for 48 h and separated into the following groups: M0-Control (untreated), M1-Control—1 $\mu\text{g}/\text{ml}$ of lipopolysaccharide (LPS; *Escherichia coli* O26:B6), PnV (14 $\mu\text{g}/\text{ml}$), F1, F2, F3 (1 $\mu\text{g}/\text{ml}$), LW-subfractions (LW-1 to LW-12) and HW (HW-1 to HW-11) (1 $\mu\text{g}/\text{ml}$). After 24 h of treatments, the macrophages were washed with PBS and used to perform the tests as described below (all tests were carried out in three independent experiments).

Phagocytosis and killing assays

Phagocytosis tests were performed by using the fungus *Paracoccidioides brasiliensis* (Pb18) or pH Red *E.coli* bioparticles (Invitrogen #P35361). For the Pb18 assay, macrophages were plated in 48-well plates at a density of 2×10^5 cells per well. After treatments, cells were incubated with the fungus for 4 h in the proportion of 1 yeast:5 macrophages per well. After incubation, cells were washed and lysed with ice distilled water to release the internalized Pb18. Then, the cell lysate containing the fungus was seeded in Petri dishes with BHI (Brain Heart Infusion) supplemented with gentamicin (96 $\mu\text{g}/\text{ml}$) and FBS (4%). After an incubation period of 7 days at 37°C , colony forming units (CFU) were manually counted. For image records, after incubation with the yeast, the wells were washed and the cells were fixed with cold methanol for 5 min and then stained with Giemsa solution for 15 min (32). The wells were washed with PBS and the images were acquired using Cytation 5—Cell Imaging Multi-Mode Reader (BioTek, Winooski, VT, USA). The killing assay was performed following the same procedure described above; however, the incubation period with the fungus was 48 h. The experiments presented in each graph were performed separated and the use of a biological material (Pb18 fungus) results in differences in the number of CFU; however, in all experiments were added the controls groups (with LPS or without any treatment).

For the bioparticle assay, macrophages were seeded at a density of 2×10^5 min cells in 24-well plates. After incubation for 2 h with 50 μg of bioparticles, the macrophages were washed extensively and immunolabelled with anti-Iba-1, as described in the morphological analysis (33). The florescence quantification (Integrated Density of Pixels) was carried out in 3–5 random photos, using the software Image J (Image Processing and Analysis in Java, version 1.39e).

Morphological analysis

After treatments, the cells were fixed with 4% paraformaldehyde for 15 min. Then, they were incubated with blocking buffer (PBS with 1% BSA, 0.3% Triton X100) for 2 h, followed by incubation with anti-Iba-1

antibodies diluted in PBS (Wako #019-19741; 1:700, overnight). Cells were washed with PBS and incubated with secondary antibodies diluted in PBS (Cy2 Goat Anti-Rabbit IgG, Jackson ImmunoResearch #111225144; 1:1,000 1h). Then, nuclei were stained with DAPI (dilution 1:1,000) (#D9542 Sigma) for 5 min and the plates were kept in a glycerol 3:1 PBS solution, at -25°C . Images were acquired in the Cytation 5 Reader. In some wells, macrophages were seeded on a coverslip and, after treatments and immunolabelling, cells were washed with PBS and the slides were mounted using fluorescence mounting medium (#F4680) to acquire qualitative images in a noninverted microscope, in high amplification. The cell count was performed in 3–5 random photos, using the Image J software (Image Processing and Analysis in Java, version 1.39e).

Cell migration analysis

The cell invasion assay was performed using transwell inserts with polycarbonate membranes of $8\ \mu\text{m}$ pore (Corning Inc., New York, NY). Macrophages in the FBS-free culture medium were added to the upper chamber of each insert (3×10^5 cells per well). The lower chamber was filled with medium supplemented with 20% FBS. Treatments were added in the upper chamber for 24 h. After that, cells that failed to migrate were removed from the upper face of the membrane using a cotton swab and the macrophages present on the lower face were stained using May-Grünwald-Giemsa. Images were acquired in an inverted microscope (Nikon Eclipse TS100; Nikon, Tokyo, Japan). The cell count was performed in 3–5 random photos, using the Image J software (Image Processing and Analysis in Java, version 1.39e).

Cytokines measure by ELISA

After treatments, the supernatants of cell cultures were collected and the enzyme-linked immunosorbent assay (ELISA) was performed for the detection of TNF- α , IL-10 and IL-6. This characterization was performed using commercial cytokines dosage kits by R&D Systems (DuoSet ELISA), according to the manufacturer's instructions. The measurements were performed in a Thermo Scientific plate reader (Multiskan Go).

Analysis of antigen-presenting parameters by flow cytometry

For the analyses of the costimulatory surface molecules, 2×10^5 macrophages/well were plated and, after 24 h with the treatments (control without any treatment, LPS $1\ \mu\text{g}/\text{ml}$, GB lysate, PnV $14\ \mu\text{g}/\text{ml}$, PnV plus GB lysate and LPS plus GB lysate), the cells were labelled with antibodies. The lysate was produced following Rainone *et al.* (34). In brief, GB NG97 cells were resuspended at 15×10^6 cells/ml and lysed by 3 cycles of freeze-thawing in liquid nitrogen. The preparation was centrifuged at 12,000 rpm for 15 min and stored in aliquots at -80°C until use. Tumour cell lysate was added at the ratio of 1 macrophage to five tumour cells. The immunostaining was performed with the following antibodies: anti-MHCII (clone M5/

114.15.2, PE-Cy7, #25-5321-82, eBioscience), anti-CD80 (clone 16-10A1, FITC, #104706, Biolegend) anti-CD86 (clone GL-1, PE, #105008, Biolegend), anti-CD40 (clone 1C10, PE-Cy5, #15-0401-82, eBioscience), anti-CD11b (clone M1/70, Alexa fluor 647, #17-0112-82, eBioscience), incubated for 30 min (4°C , in a dark chamber). The cells were then fixed with paraformaldehyde 1% for 30 min and 10,000 events were acquired using the Flow Cytometer (BD FACSVerser). The data were analysed by FlowJo VX software. For this experimental design, cytokines (IL-6, TNF- α and IL-10) were also dosed by ELISA, as described in this topic.

Macrophages and glioblastoma (NG97) coculture

Macrophages were plated at a density of 3×10^5 cells per well in 24-well plates; after 24 h with treatments, the stimuli were removed and the macrophages were washed and incubated with 3×10^5 glioblastoma (NG97) cells. The coculture was maintained for 24 h and, after this period, the procedure for assessing cell viability was performed through the labelling of live cells with DAPI. The analyses were made by flow cytometry or image acquisition in Cytation-5. Anti-Iba1 was used to identify macrophages to differentiate from tumour cells. The fluorescence quantification (Integrated Density of Pixels) was carried out in 3–5 random photos, using the software Image J (Image Processing and Analysis in Java, version 1.39e).

Statistics

The data analysis was made by GraphPad Prism software (v. 5.0 GraphPad, San Diego, CA). The level of significance was evaluated using one-way analysis of variance followed by Dunnett's multiple comparisons test. Unpaired Student's *t*-test was used to compare each treatment with the control. Data are presented as mean \pm standard error of the mean. $P < 0.05$ indicated statistical significance. All experiments were performed two or three times independently with three replicates in each group.

Results

In order to contribute to the investigation of the therapeutic implications of the use of natural compounds for drug discovery, in this section, we describe the results of the experiments performed with the main objective of evaluating the effects of PnV and its purified components on the modulation of macrophages, with the perspective of selecting the subfraction responsible for the most pronounced effects.

Verification of venom quality and purification in sub-fractions by HPLC

Figure 1A shows that the standard and quality of the venom sample was as previously reported (23, 25). The first procedure for separation of the crude venom into fractions was carried out by molecular mass criteria, using molecular filters with nominal separation at 10 and 3 kDa, according to Santos *et al.* (23). Three main fractions were obtained: F1 (LW, $<3\ \text{kDa}$), F2 (intermediate weight, between 3 and 10 kDa) and F3

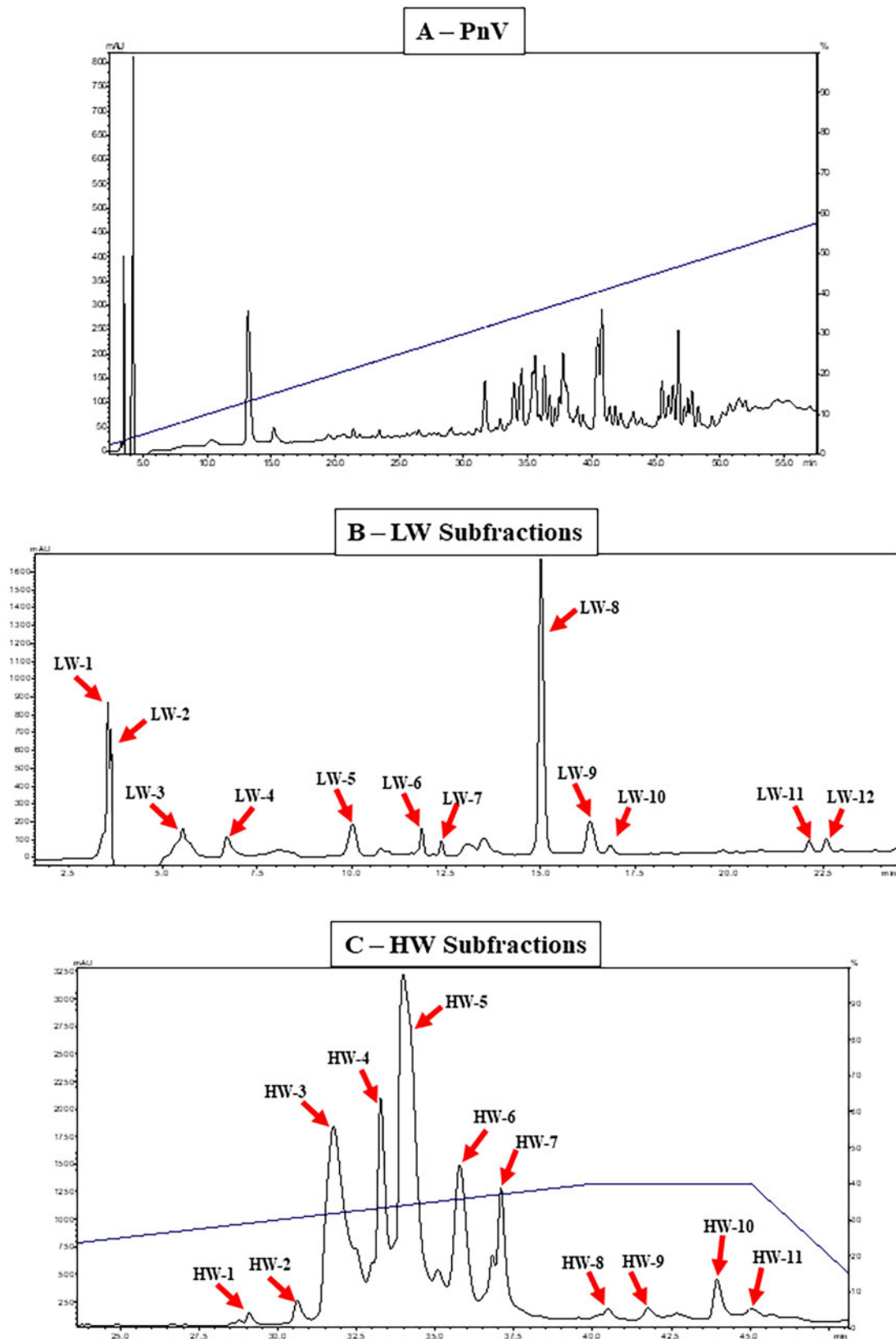


Fig. 1. Venom quality and purification in subfractions by HPLC. Graph A shows the standard and quality of the venom sample. Graphs B and C show the purification of F1 + F2 (LW) and F3 (HW) by HPLC, respectively, generating 12 LW-subfractions (LW-1 to LW-12), and 11 HW-subfractions (HW-1 to HW-11).

(HW, above 10 kDa). These fractions are still complex mixtures and were evaluated as described below to select those with the most significant effects on macrophages. Taking all the obtained results together, F2 and F3 were considered more effective in most parameters; however, F1 had a significant effect in the killing assay. Therefore, all fractions were purified again to continue the study. **Figure 1B and C** shows the purification of F1 and F2 together (now referred to as LW) and F3 (now referred to as HW) by HPLC, respectively. This procedure generated 12 LW-subfractions, named LW-1 to LW-12, and 11 HW-subfractions, named HW-1 to HW-11. These PnV components have been tested for macrophages immunomodulation, as reported below.

Crude venom and its fractions and subfractions activity on macrophage phagocytose

In the phagocytosis assay with the fungus Pb18, fractions F2 and F3 significantly increased the number of CFUs (**Fig. 2.1A**), while the number of yeast cells in suspension after lysis of macrophages was increased only in F2 (**Fig. 2.1B**), demonstrating that F2 and F3 were the fractions with higher potential to activate macrophages. Of note, all other treatments appeared to increase the phagocytic activity, but not significantly (**Fig. 2.1**).

Figure 2.2 shows microscopic images of macrophages incubated with Pb18. It is possible to observe that macrophages treated with LPS, PnV and fractions (mainly F2 and F3) present more intracellular fungi (see detail in the highlighted panel G) compared to the control. These data confirm that groups treated with venom and fractions, similar to LPS (M1-control), induced higher phagocytosis capacity when compared to the untreated control (M0-control). An accurate observation reveals that F1 was very similar to M0-control, PnV and F3 induced more phagocytosis than F1 and M0, and LPS (M1-control) and F2 were greater than other groups.

The Pb18-phagocytosis assay was also performed with the subfractions purified from F1 + F2 (LW) and F3 (HW). Subfractions LW-2, -3, -5, -10, -11, -12 (**Fig. 2.3A**) and HW-1, -2 and -3 (**Fig. 2.3B**) induced a significant increase in phagocytosis compared to control. Although several subfractions have shown an effect on phagocytosis and killing (shown below), from overlapping these results, the following subfractions were chosen as the best to continue: LW-9, -11, -12 and HW-2, -3, -6; in addition, LW-6 was chosen as a control of fraction with no relevant effect.

The results obtained with *E.coli* bioparticles (**Fig. 3**) were compatible with those observed with the fungus. **Figure 3.1** shows that PnV, F2 (not significant) and F3, as well as LPS, increased phagocytosis when compared to the M0-control, while F1 was very similar to untreated cells. Fluorescence quantification is shown in graph M. When the selected subfractions were tested (**Fig. 3.2**), it was possible to observe that LW-9 (panels G and H) had the best effect, which was statistically significant (graph S).

Macrophage Pb18 killing ability by PnV, its fractions and subfractions stimuli

In the killing assay, treated cells were incubated with the fungus Pb18 for a prolonged period (48 h) to allow them to eliminate the pathogen. Then, cells were washed and lysed, and the supernatant was cultured to evidence alive fungi. The less Pb18, the increased killing capacity. In graph 4.A, the results demonstrate that PnV, as well as LPS, increased intracellular death compared to control. The fractions also increased the killing of the fungus, especially F1 and F2.

The tests with subfractions (**Fig. 4B and C**) showed that LW-9, -11, -12 (graph B) and HW-6, -8, -9 (graph C) were the subfractions with increased fungi killing capacity. Interestingly, LW-1, -2 and -3 decreased the ability of macrophages to kill the fungus.

Macrophage morphological alterations under venom, its fractions and subfractions treatment

Cell morphology was analysed by immunofluorescence label of Iba-1, a macrophage marker (green), and DAPI to highlight the nuclei (blue) (**Fig. 5**). Iba1 is recognized as a pan-macrophage marker and its expression is increased when these cells are activated (**35, 36**). Iba-1 staining demonstrated that the cells generated from bone marrow were successfully differentiated in macrophages (that was also confirmed by the CD11b staining detected by flow cytometry, as described later) (**Fig. 5**).

Figure 5.1 shows that the cells treated with PnV had increased processes, were multinucleated and with increased cytoplasm, when compared to the M0-control, a profile characteristic of activated macrophages (more clearly visible in the panels with higher amplification—B, D, F, H, J, L). The same aspect was observed for the group treated with LPS, in which the cells were even larger. Fractions F2 and F3 (mainly F3) induced a morphology very close to PnV and LPS.

In addition, the images with lower amplification in **Figure 5.1** (panels A, C, E, G, I, K) clearly suggest an increase in the number of cells, comparing all treatments with M0-control. Considering that in all groups there was initially the same number of cells, this result suggests that PnV and fractions could be stimulating cell proliferation. In fact, graph M shows that all treatments (mainly LPS, PnV and F1) significantly increased the cell count compared to M0-control.

Figure 5.2 shows the same analysis, using subfractions. LW-9 (panel D) and HW-3 (panel H) induced the most activated morphology of macrophages. LW-6, -11 and HW-2 induced the most discrete morphological alteration, being similar to M0. Graph J shows that there is no significant difference between the groups in cell count.

Stimulation of macrophage migration by the crude venom, its fractions and subfractions

The cell migration assay was performed for 24 h of exposure to treatments, using plates containing transwell inserts. **Figure 6.1** shows that all treatments increased macrophage migration when compared to M0-control. Interestingly, LPS (M1-control) did not

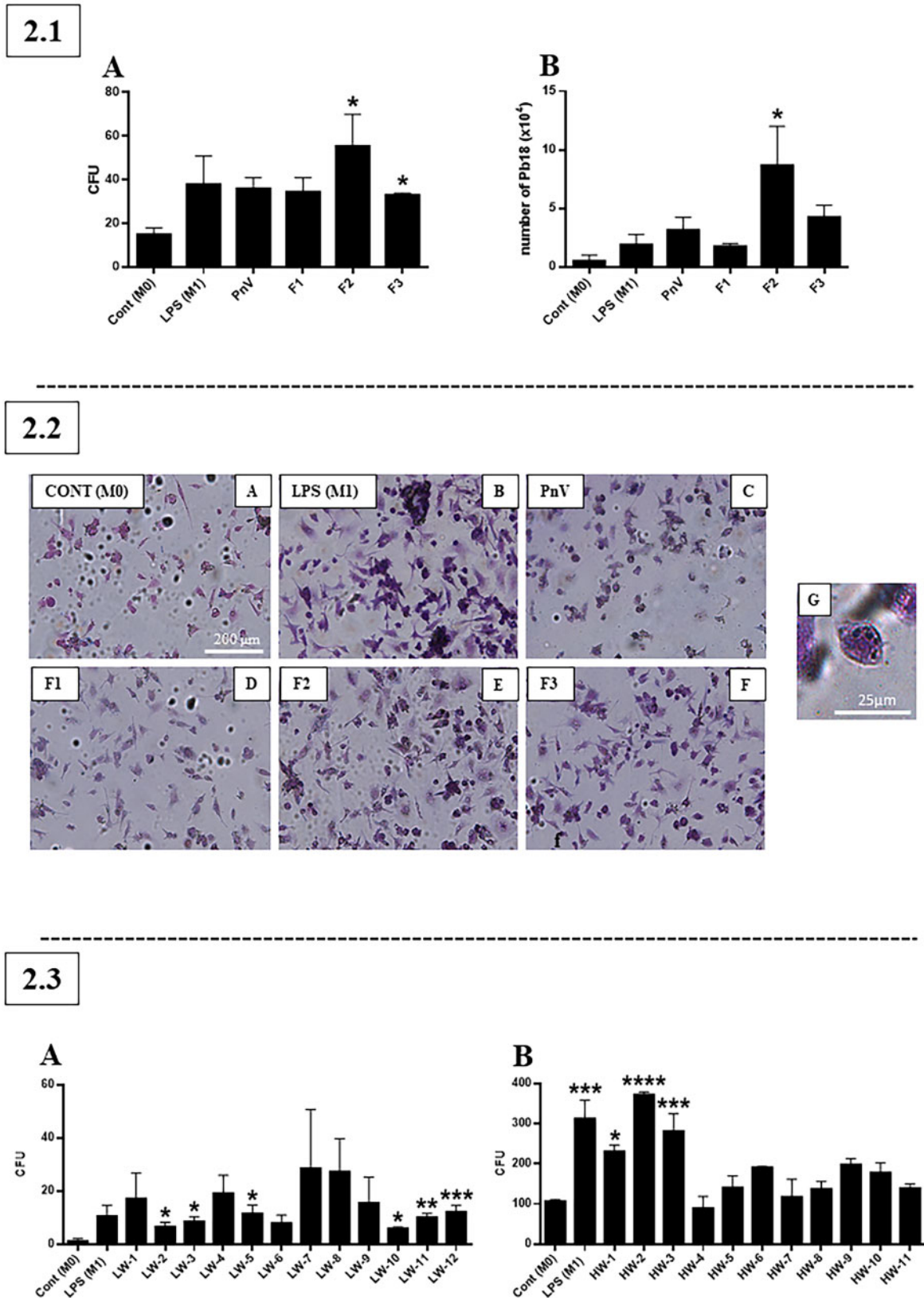


Fig. 2. Phagocytosis of *Paracoccidioides brasiliensis* (Pb18) fungus by macrophages. (2.1) The first screening with PnV, F1, F2 and F3. (2.A) The capacity of phagocytosis by each group was evaluated by the number of CFU after the period of incubation (7 days) with the fungi in the BHI medium. (2.B) Number of fungi after the lysis of the macrophages, this is another quantitative way to evaluate the number of fungi that were phagocytosed. G: Highlight of figure B of the group with LPS in the 2.2 panel showing a bone marrow macrophage (purple) with the fungi phagocytosed (black points). Macrophages were more phagocytic when pretreated with LPS (M1), PnV, F2 or F3 (less significantly with F1), compared to untreated cells (M0). (2.2) Microscopic images of macrophages incubated with Pb18; PnV and fractions (mainly F2 and F3) showed more intracellular fungi (highlighted in panel G), compared to the control. (2.3) Demonstrates that phagocytosis was increased with the subfractions LW-2, -3, -5, -10, -11, -12 and HW-1, -2, -3. * $P < 0.05$, ** $P < 0.01$, *** $P < 0.001$, **** $P < 0.0001$, compared to the control (M0).

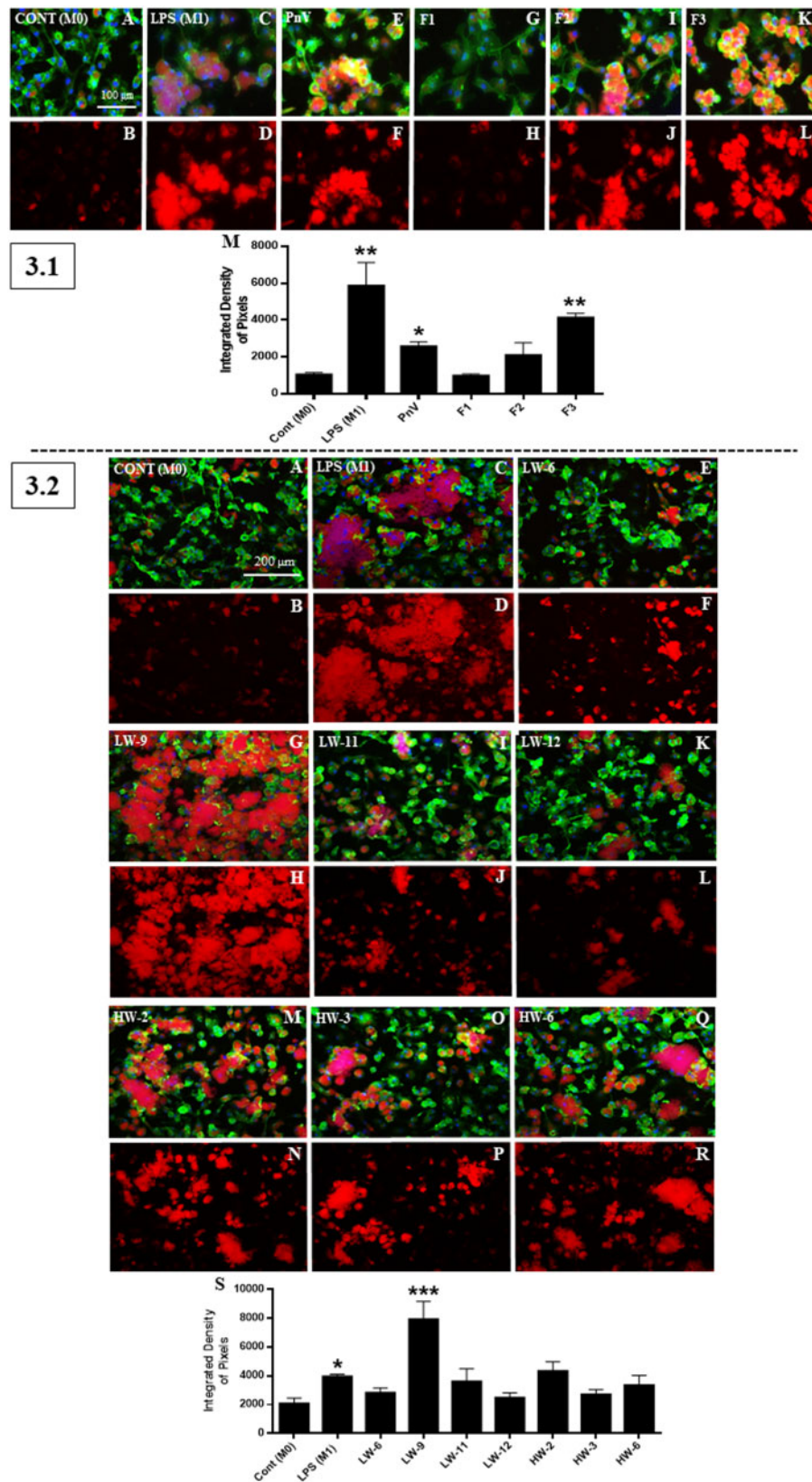


Fig. 3. Phagocytosis assay using *E.coli* bioparticles. The green fluorescent label on macrophages corresponds to Iba-1, and the bioparticles are the red fluorescence. The pictures above on each panel show the double labelling and the pictures below show only the phagocytized bioparticle. (3.1) LPS, PnV, F2 (not significant) and F3 induced greater phagocytosis capacity when compared to the M0-control, while F1 was very similar to untreated cells (quantification demonstrated in the graph M). (3.2) LW-9 (panels G and H) had the best effect (quantification demonstrated in the graph S). * $P < 0.05$, ** $P < 0.01$, *** $P < 0.001$, compared to the control (M0).

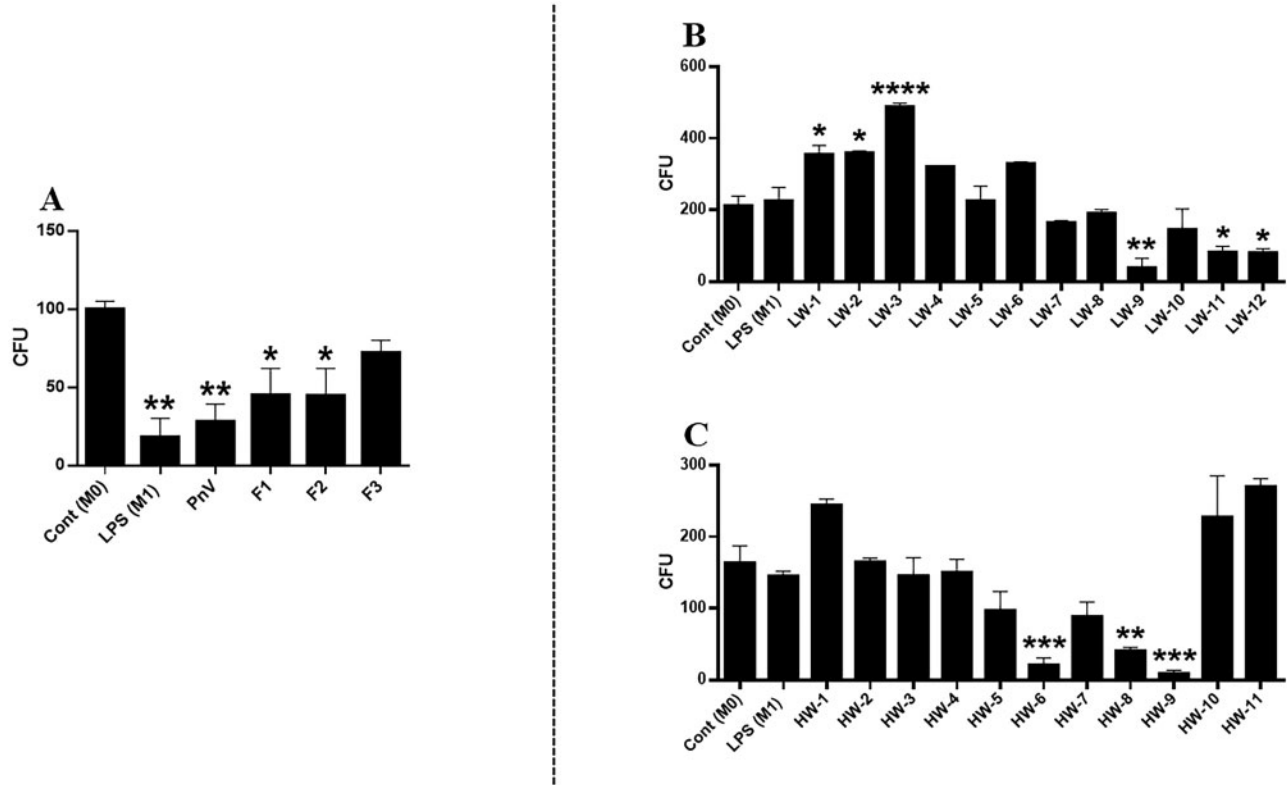


Fig. 4. Killing assay of *Paracoccidioides brasiliensis* (Pb18) fungus by macrophages, where reduced CFU number refers to the increased killing capacity and vice versa. Graph A shows that PnV, LPS, F1 and F2 significantly increased the killing of fungi. Graphs B and C demonstrate the results of subfractions isolated from F1 + F2 (LW) and F3 (HW), respectively. LW-9, -11, -12, and HW-6, -8, -9 had the best effects, inducing a greater ability of macrophages to kill fungi. * $P < 0.05$, ** $P < 0.01$, *** $P < 0.001$, **** $P < 0.0001$, compared to the control (M0).

induce much migration, while PnV and fractions F2 and F3 increased it. It is also clear that in the groups treated with venom and fractions, especially PnV, cells have large and thin stretches, possibly the mechanism by which they can pass through the pores. This aspect was also observed in the morphological analysis by Iba-1 labelling.

Figure 6.2 demonstrates that all subfractions increased the migration of macrophages, but LW-9 and HW-2 were more efficient. The cell morphology was different depending on the subfraction; treatment with LW-9 and HW-2 induced cells with long processes and thin body. On the other hand, HW-3 and, more pronounced, HW-6, showed cells with a large and rounded body, without (or with few) processes.

Venom, fractions and subfractions effects on cytokines release

To better understand the functional profile of macrophages treated with PnV components, pro- and anti-inflammatory cytokines were measured in the culture supernatant.

Figure 7.1 shows that LPS (M1-control) significantly increased the release of pro- (IL-6 and TNF- α) and anti-inflammatory (IL-10) cytokines, corroborating the literature (37). On the other hand, the venom and all fractions did not alter any of those molecules when compared to the control. These data suggest that the venom activates macrophages for a different profile rather than the classic M1. This atypical and specific profile were referred to as M-PnV.

Figure 7.2 demonstrates that a similar result was observed for the subfractions, where none of them, induced TNF- α expression. However, LW-1 and LW-9, as well as LPS, significantly increased IL-10 release (graph B).

Action of PnV, fractions and subfractions on molecules involved in antigen presentation by macrophages

Considering that macrophages present antigens, this ability was assessed to verify whether the venom and its components could alter that function. For that, macrophages were pulsed with GB cell lysate, concomitantly to the treatment with LPS or PnV. Only lysate or the treatments alone were also evaluated. Figure 8A–E shows the main molecules involved in the antigen presentation. In general, LPS (mainly) and lysate alone were able to induce this function in macrophages, while PnV had no effect.

CD11b expression was significantly increased by LPS and lysate (graph A), but not by PnV. When concurrent exposures of PnV plus lysate or LPS plus lysate were performed, this molecule was increased, allowing to infer that the stimulation was not due to the venom components, but to the presence of GB antigens in the lysate. Similar results were observed for CD80 and MHCII (graphs B and C). For the costimulatory molecules CD40 and CD86 (graphs D and E), only LPS induced a significant increase.

Cytokines release in the supernatant was also evaluated in this experimental design (Fig. 8 graphs F–H).

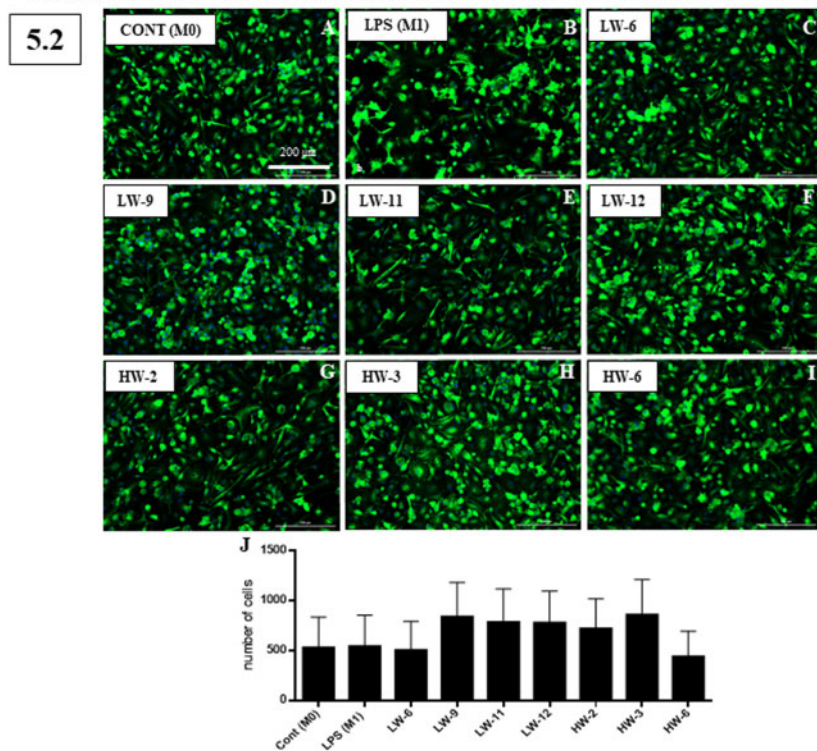
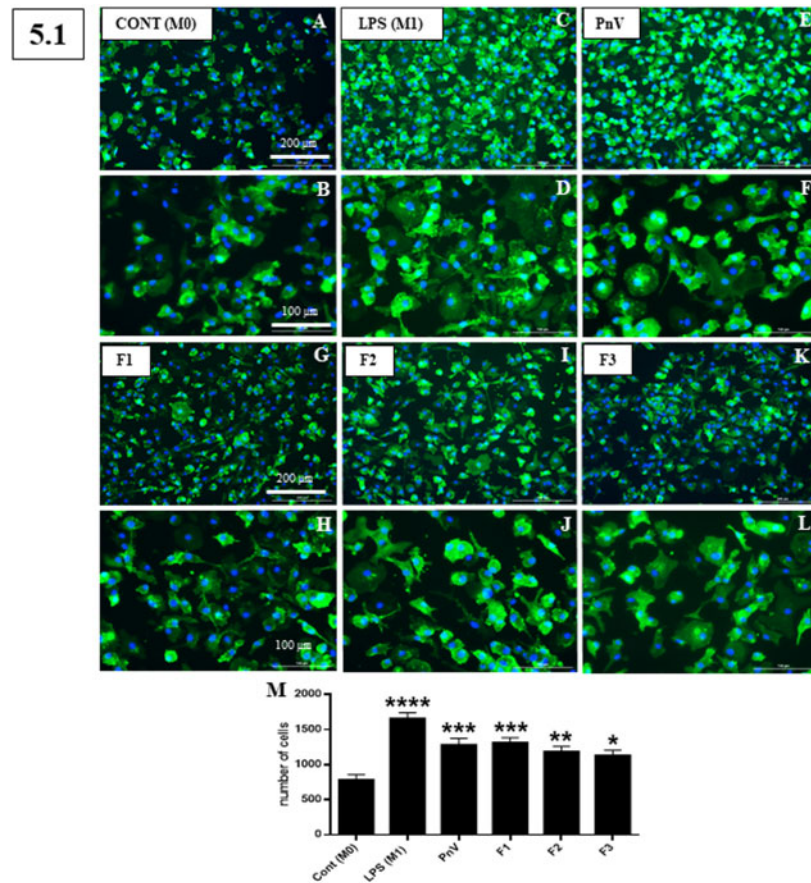


Fig. 5. Macrophage morphology analysis: immunolabelling for Iba-1 (green) and DAPI to highlight the nuclei (blue). Panel 5.1 shows that macrophages treated with PnV and fractions F2 and F3 exhibited a morphological profile similar to M1-control (LPS), with long processes, increased cytoplasm and multinucleated cells. The cell count (graph M) revealed that all treatments significantly increased the number of cells compared to M0. Panel 5.2 demonstrates that, among subfractions, LW-9 and HW-3 induced the most activated morphology; however, there was no significant difference when cells were counted (graph J). Scale bars: 5.1 upper panel, 200 μm; 5.1 lower panel, 100 μm; 5.2, 200 μm. * $P < 0.05$, ** $P < 0.01$, *** $P < 0.001$, **** $P < 0.0001$, compared to the control (M0).

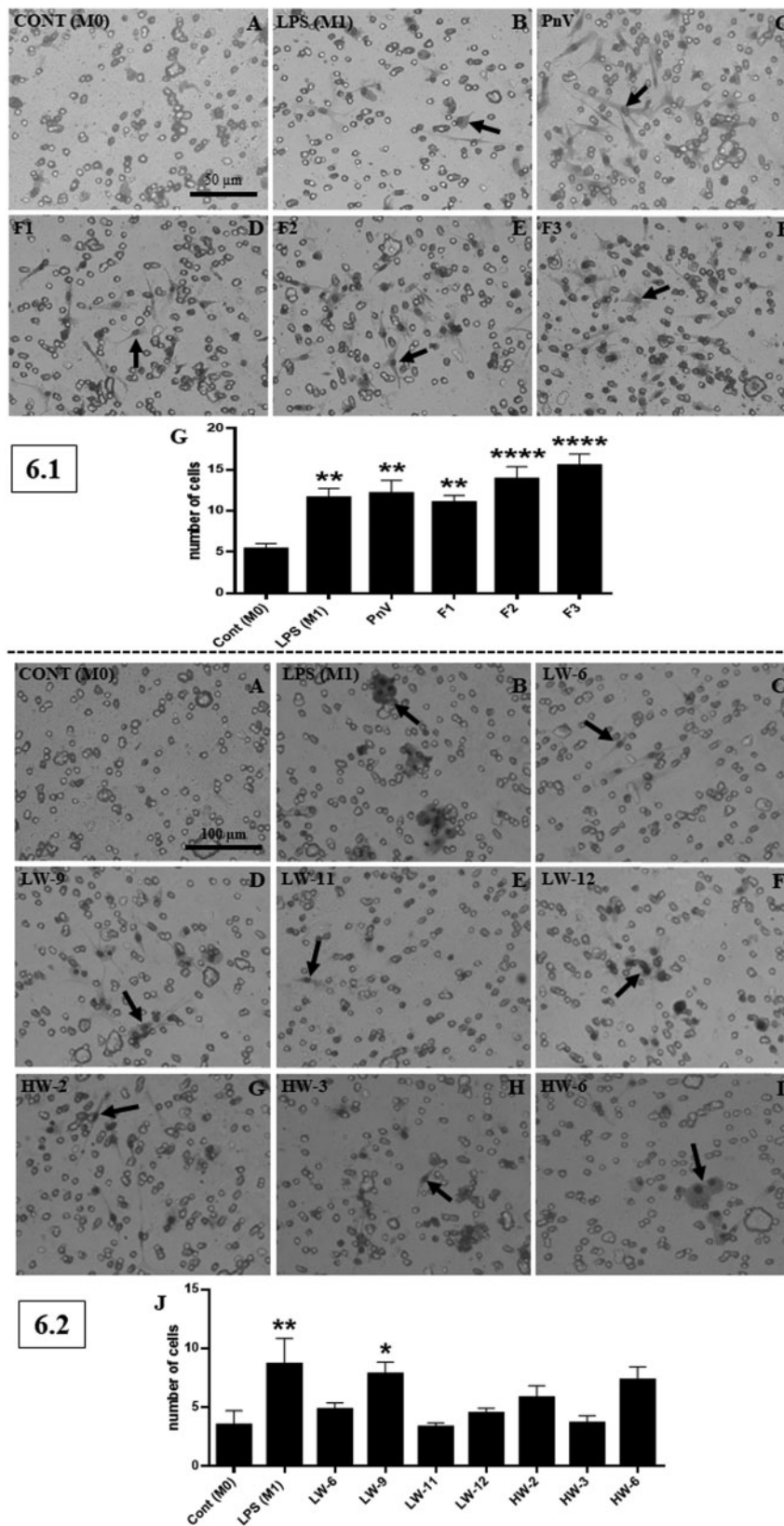


Fig. 6. Cell migration assay using transwell. Panel 6.1 shows that all treatments significantly increased macrophage migration compared to M0-control (A); F2 (E) and F3 (F) had the best effect (cells count showed in graph G). Panel 6.2 demonstrates that, among subfractions, LW-9 (D) induced significantly increased migration (cell count presented in graph J). The pictures also show that LW-9 and HW-2 induced cells with long processes and thin body, while HW-3 and, more pronounced, HW-6, showed cells with a large and rounded body, without (or with few) processes. The arrows point to the cells. * $P < 0.05$, ** $P < 0.01$, **** $P < 0.0001$, compared to the control (M0).

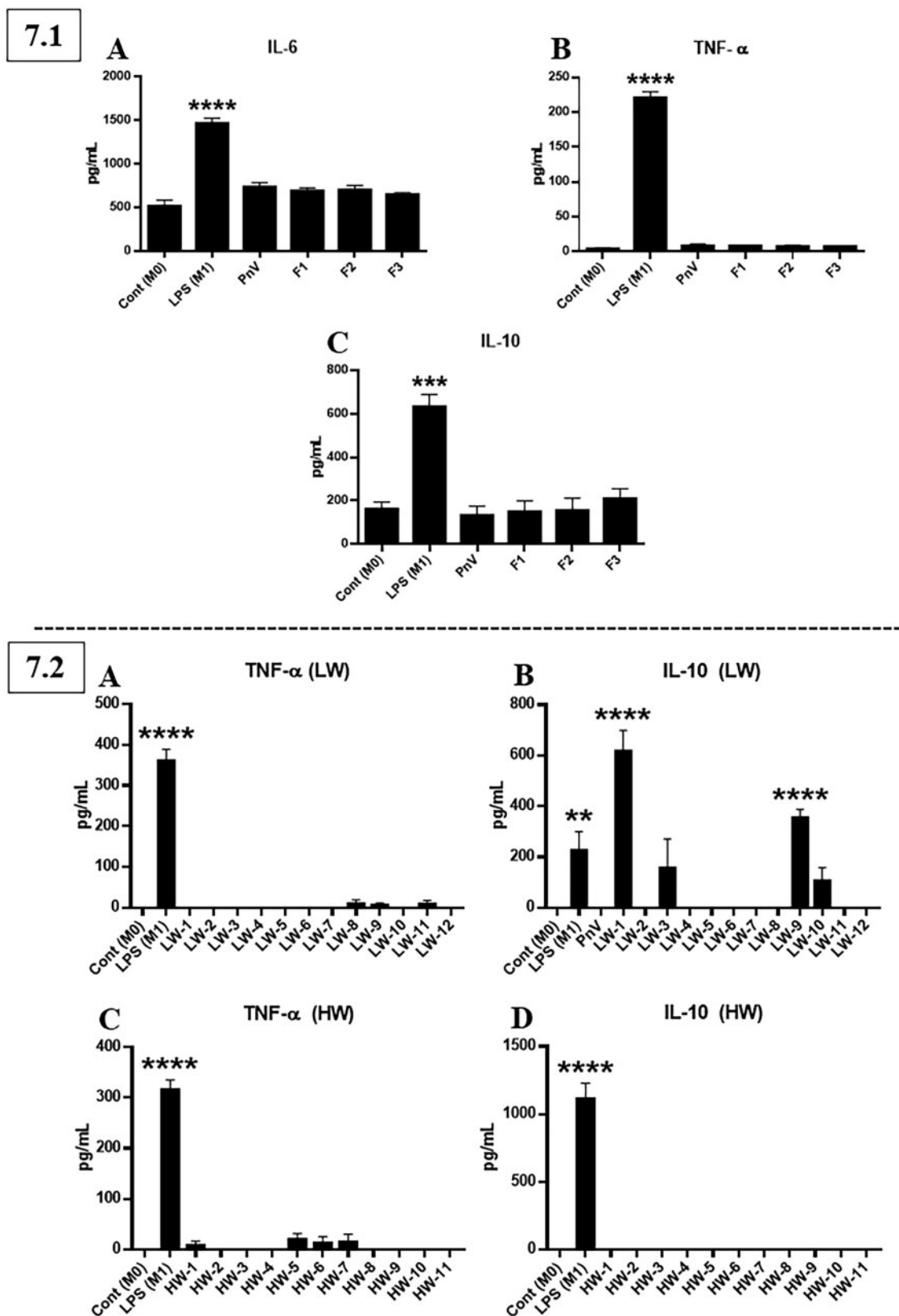


Fig. 7. Quantification of cytokines released in the culture supernatant by ELISA. Graphs in 7.1 show that LPS strongly increased IL-6 (A), TNF- α (B) and IL-10 (C), while PnV, F1, F2 and F3 did not alter the release of any evaluated cytokines. Graphs in 7.2 demonstrate that LW (A and B) and HW-subfractions (C and D) did not induce cytokines, excepting LW-1 and LW-9 (B), which increased IL-10. ** $P < 0.01$, *** $P < 0.001$, **** $P < 0.0001$, compared to the control (M0).

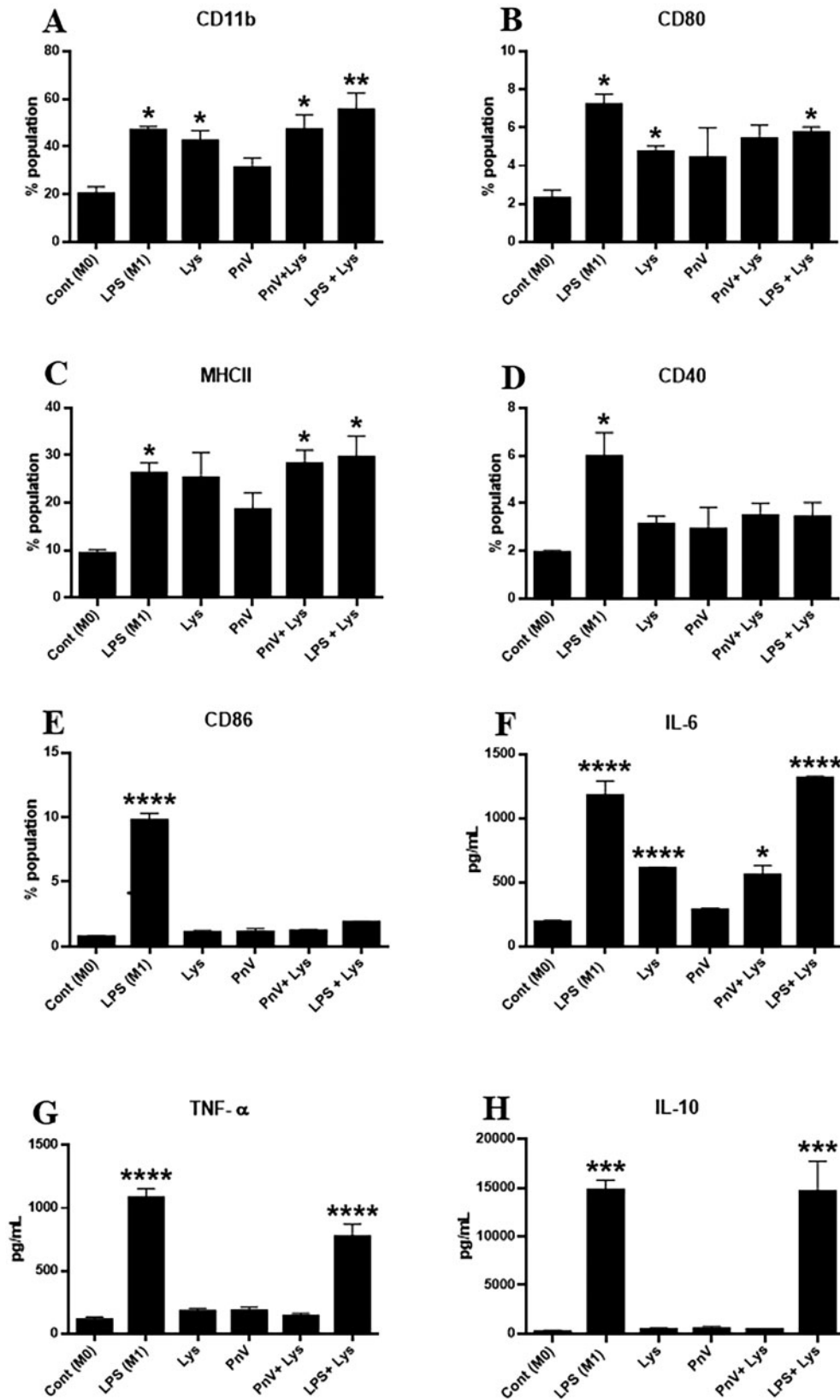


Fig. 8. Flow cytometry analysis of costimulatory molecules involved in antigen presentation (graphs A–E) and cytokines dosage in the supernatant by ELISA (F–H). For this experiment, macrophages were pulsed with glioblastoma (NG97) cells lysate, concomitantly to the treatment with LPS or PnV. The treatments alone were also evaluated. Lysate and LPS, alone or combined, increased CD11b (A), CD80 (B) and MHCII (C). PnV plus lysate also increased the molecules, but this effect is obviously due to the lysate since PnV alone had no effect. CD40 (D) and CD86 (E) were modulated only by LPS. IL-6 (F) was upregulated by LPS and lysate, alone or combined with LPS, and PnV plus lysate also increased this cytokine, but not PnV alone. TNF- α (G) and IL-10 (H) were increased only by LPS with or without lysate. * $P < 0.05$, ** $P < 0.01$, *** $P < 0.001$, **** $P < 0.0001$, compared to the control (M0).

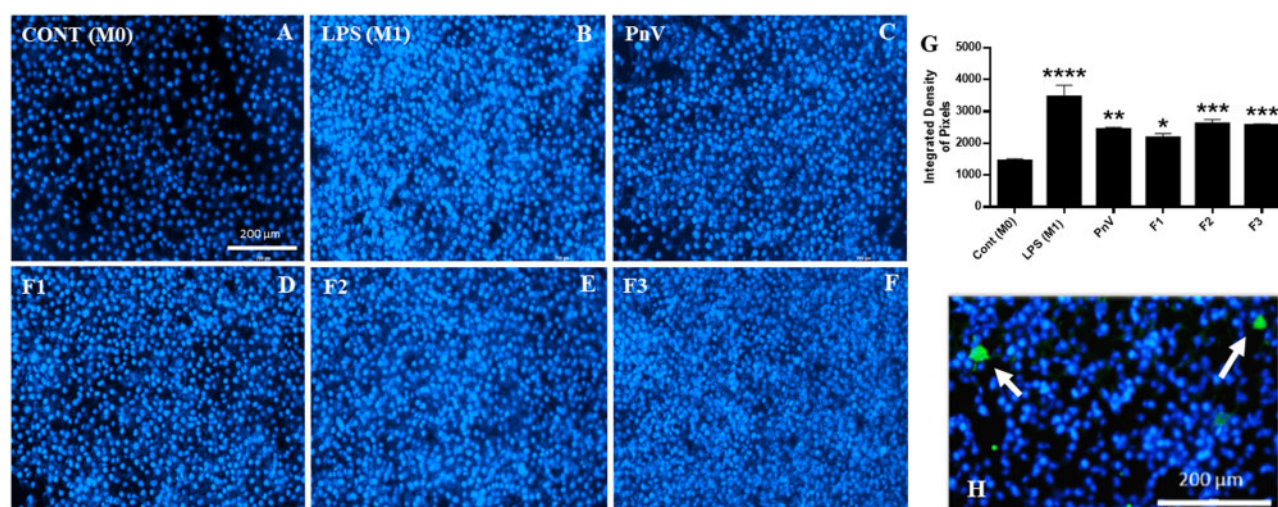


Fig. 9. Glioblastoma (NG97) cells viability with DAPI labelling in unfixed cells. A coculture was performed with macrophages and GB cells. The macrophages were previously stimulated with LPS, PnV, F1, F2 or F3. Panels A–F demonstrate the DAPI fluorescence (blue nuclei), corresponding to dead cells. All treatments (B–F) increased the fluorescence intensity compared to the control (A). Macrophages treated with LPS, F2 and F3 (panels B, E and F, respectively) were apparently more efficient in killing tumour cells than PnV (C) and F1 (D). Graph G shows the statistical difference in fluorescence quantification. The picture in detail (H) shows the macrophages labelled with Iba-1 (green; indicated by arrows), demonstrating that the nuclei labelled with DAPI are mainly GB cells and not macrophages. * $P < 0.05$, ** $P < 0.01$, *** $P < 0.001$, **** $P < 0.0001$, compared to the control (M0).

The results confirmed that the PnV and fractions did not induce cytokines release. Graphs F and G show that only LPS increased the levels of TNF- α and IL-10, while the lysate, PnV and PnV plus lysate had no effect. IL-6 release (graph H) was increased by LPS, lysate and LPS plus lysate, while PnV had no effect. The treatment with PnV plus lysate induced an increase in this cytokine, but this is due to the lysate stimulation *per si*.

PnV and its fractions were efficient in activating macrophages to kill tumour cells

Finally, it was necessary to confirm whether the specific macrophage profile induced by PnV components, which can phagocyte and kill Pb fungus, presents an activated morphology, can migrate more efficiently, but does not release cytokines and does not present antigens, would be able to kill tumour cells. For this, a coculture with macrophages and GB cells was performed. The macrophages were previously stimulated with LPS, PnV, F1, F2 or F3.

The viability of tumour cells was assessed by DAPI labelling in living cells. The principle of the method is that DAPI is predominantly impermeable to living cells, what allows it to be used as a viability dye in unfixed cells to discriminate intact cells and cells with compromised membrane.

Figure 9 demonstrates that all treatments increased the DAPI fluorescence, suggesting that there is a greater number of dead cells, when compared to the control. Macrophages treated with LPS, F2 and F3 (panels B, E and F) were apparently slightly more efficient in killing tumour cells than PnV and F1. Graph G shows the difference observed when fluorescence quantification was performed.

It is clear, therefore, that PnV and, even more expressively, fractions F2 and F3 have components

capable to activating macrophages, increasing their antitumour ability.

Discussion

Natural products are an important tool for the development of drugs represented by 35% of medicines that come from natural sources. The greatest biodiversity of the world is located in Brazil and Brazilian scientists have published scientific evidences of the potential of plants and venoms in the development of drugs. The development of new therapies to treat cancer is challenging; specifically, for GB, which about 85% of therapies fail in early clinical trials (38). Natural products can represent an alternative for the development of new antineoplastic drugs. Since the 1980s, 174 new compounds were approved to be commercialized for cancer treatment and, among them, 93 (53%) were natural products or derivatives directly or based on natural sources (39).

A series of studies by our group have shown that the venom of *P.nigriventer* (PnV) has antitumour properties. PnV components had a direct effect on GB cells *in vitro*, reducing viability and proliferation, arresting the cell cycle in G0, inducing cell death (23) and decreasing cell migration and adhesion (25). In addition, PnV impaired GB progression in an *in vivo* murine model, with a concomitant modulation of circulating immune cells, increasing monocytes in the blood; also, the venom induced an augment in the macrophages infiltrated in the tumour (24). However, some questions remained open: whether the infiltrated macrophages were being modulated by the components of the venom and if these immune cells were contributing to the effect of PnV on tumour progression.

The present findings showed that the venom induced greater phagocytosis and killing activity,

promoting an activated morphological profile, and increased migration. On the other hand, interestingly, the venom did not alter the release of cytokines and could not induce the expression of molecules involved in the presentation of antigens. Finally, macrophages preactivated with PnV were able to kill cancer cells more efficiently than M0-control. The results also showed that purified fractions and subfractions of the venom have different effects on macrophages. This is expected, since the venom is a very complex mixture of heterogeneous molecules. F2 and F3 were better than F1 in immunomodulatory effects and were chosen to be purified again. A total of 23 subfraction were obtained and 7 of them (LW-9, -11, -12 and LW-2, -3, -6) were selected as the most effective to continue the tests. The results suggest that LW-9 demonstrated the most efficient immunomodulatory effects and can be an effective immunoadjuvant, improving the response of macrophages in the treatment of GB. LW-6 was chosen from the first screening as a control of a subfraction with no effect; the next experiments confirmed that this subfraction was not able to immunomodulate macrophages.

The data of the present study revealed that M0 cells had a slight capacity for phagocytosis and killing, while M1 demonstrated a high capacity to do so. The results showed that components present in the venom were able to modulate macrophages to an activated profile capable of phagocytosing bioparticles and Pb18 fungus. In addition, PnV components could kill the yeast more than M0 cells. This is an important test to assess the functional activity of macrophages, considering that this is one of the main functions performed by these cells (40). The findings also show that the PnV components that induced phagocytosis were not necessarily the same as those that induced death. Furthermore, it is possible that molecules from PnV have synergistic and antagonistic effects, considering that, when separated, the fractions and subfractions were less or more efficient than the whole venom.

Taking these results and considering that the use of molecules that increase the functions of killing and/or phagocytosis can be a strategy to fight cancer (17, 20, 21), other experiments were carried out to confirm whether the components of the venom could be strategic tools to modulate macrophages. The analysis of morphology has been recognized as a robust and important biomarker for assessing cell function (41). The activated profile of macrophages treated with PnV components was confirmed by the morphological observation, which shows that the cells were larger, with multiple nuclei and with long and slender processes, similar to the M1-control phenotype. Apparently, PnV components, as well as LPS, induced macrophages proliferation. Another important parameter analysed was the macrophage migration capacity. The migration test is defined as the movement of cells through a membrane in order to analyse chemotactic responses (42). Results published by our group demonstrated that the tumours (GB) from mice treated with PnV have more infiltrated macrophages (24). The present findings corroborate those results, showing that PnV

components, mainly LW-9, induced greater macrophages migration. Interestingly, Santos *et al.* (23) and Barreto *et al.* (25) showed that PnV decreased the migration of GB tumour cells *in vitro*, and F1 was the main fraction implicated in this effect. In the present work, we showed that F2 and F3 were able to increase macrophages migration, indicating that PnV components have different actions that may depend on the type of cell (target), as well as the venom molecule.

Although all so far discussed parameters discussed so far suggest that the components of the venom induce a macrophage profile very similar to M1, the release of cytokines results demonstrated that in fact it is not the same phenotype. The M1 macrophage (LPS-control) increased the three cytokines analysed: IL-6 and TNF- α (proinflammatory) and IL-10 (anti-inflammatory). On the other hand, PnV, its fractions and subfractions did not alter them, except LW-1 and LW-9, which increased IL-10. It is well known that M1-macrophages, classically activated by LPS and IFN- γ , are characterized by the production of proinflammatory cytokines, such as IL-6 and TNF- α , and also iNOS, in murine macrophages (43). Thus, we can infer that the profile of the cells treated with the venom is not an M1, but a specific phenotype, named M-PnV macrophages. The specific features and consequences of such phenotype will be investigated in further studies.

Even though M1 is described as an antitumour macrophage, there is a consistent literature that clarifies that, regardless of its polarization, TAMs with anti- or proinflammatory phenotype are related to a worst prognosis in many types of cancer (44). Recent literature has shown that M1 macrophages may be associated with a poor tumour prognosis, and this effect is specifically related to the release of TNF- α (45). Moreover, another important point is that therapies with proinflammatory cytokines or that induce an increase in their release have the potential to promote autoimmune diseases as an adverse effect, such as multiple sclerosis, rheumatoid arthritis, type 1 diabetes and inflammatory bowel disease (46). Therapies with TCR-T and CAR-T cells mediate the release of cytokines, with the consequent risk of developing cytokine release syndrome (10, 11). Also, immunotherapy in general, including checkpoint blockers, may cause autoimmune diseases, *e.g.* pneumonia and colitis (47). Therefore, LW-9 induces a macrophage that has the ability to phagocyte, kill and migrate more, but has caused no proinflammatory cytokine release, while releasing IL-10, which can be an important balance of immune modulation. This specific macrophage phenotype appears to be an important tool for the development of a new immunoadjuvant not based on cytokines or antibodies, with less chance of autoimmune reactions.

Considering that the macrophage is known to be a multifunctional antigen-presenting cell (48), this ability was also evaluated to understand the immunomodulatory mechanisms of PnV components. Results showed that, while LPS and tumour cell lysate improved this function, the venom was unable to modulate.

Finally, even though PnV is capable of modulating macrophages for an active phenotype, it was important to assess whether this specific profile induced by PnV components could kill tumour cells, since the evasion of the immune system by tumour cells is well known as one of the key points in the failure of immunological response (49). The coculture of macrophages, preactivated with the venom and fractions, with tumour cells showed that M-PnV macrophages decreased the viability of tumour cells more efficiently than M0 macrophages, as demonstrated by the entry of DAPI into GB cells. The M-PnV function was very similar to the expected effect of M1 macrophages (LPS-control) (50, 51).

Therefore, it is possible to conclude from the present findings that PnV components, mainly LW-9, are capable of activating macrophages against tumour cells, and the mechanisms behind this effect appear to be the modulation of phagocytosis without altering cytokines release and antigen presentation. One question that remains unanswered is how the components of the venom do it. Some mechanisms for inhibiting phagocytosis in cancer have recently been taken into account in the literature. For example, the inhibition of the engulfment by macrophages through cluster of differentiation 47 (CD47) (52). CD47 is a transmembrane molecule, probably expressed in all types of cancer cells, which has a role in macrophages and dendritic cells, through the signal regulatory protein- α (SIRP α) (53). Through overexpression of CD47 on its surface, cancer cells defend themselves against macrophages phagocytosis (47, 54). Blocking the CD47-SIRP α interaction by monoclonal antibodies vigorously awakens the innate immunity in mice (55). Furthermore, the leukocyte immunoglobulin-like receptor B1 (LILRB1) on the surface of TAMs has been shown to bind to a portion of MHC-I in cancer cells, which inhibited the ability of macrophages to engulf them. *In vitro* and *in vivo* analysis showed that blocking the MHC-I and LILRB1 pathways stimulated macrophages, increasing the engulfment, and significantly delayed tumour growth in mice (56). Therefore, the inhibitory signals of phagocytosis by CD47-SIRP α and MHC-I-LILRB1 can be potential targets for the components of the venom, and these mechanisms will be evaluated in future studies.

Conclusion

Taken together, these results suggest that PnV components, specifically present in LW-9, may be new immunoadjuvants to modulate macrophages, increasing phagocytosis without inducing the release of proinflammatory cytokines. The inhibition of macrophage-mediated phagocytosis is an essential mechanism for the immune evasion of the tumour; therefore, agents targeting macrophages, which have recently received attention and been developed, can be important tools for cancer treatment. The investigation of the detailed mechanisms of LW-9, and the characterization of its biochemical structure, is underway to develop a new noncytokine and nonantibody immunoadjuvant to treat cancer.

Data Availability Statement

The authors declare that all data will be available, if necessary.

Author Contribution Statement

J.M. performed most of the experiments, including macrophages generation, phagocytosis and killing, morphology and migration tests; G.P. and J.O. helped in the experiments with Pb fungus; A.M. maintained the cells and helped in all experiments; T.A.A.R.S. and R.S. extracted venom from the spiders and purified the samples; R.T. received J.M. for an internship and provided training in macrophages generation, in addition to assisting in the improvement of the manuscript; A.L.B. contributed with his expertise in immunology, conducting the experiments and revising the manuscript; N.B. helped with the immunofluorescence method; G.M.C. and E.G. contributed with their experience with cancer and revised the manuscript; J.L.V.A. contributed with his expertise in brain cancer by revising the manuscript; L.V. contributed with her expertise on immune system, interpreting the results. C.R. conducted the study, performed the experimental design, interpreted the results and drafted the manuscript. All authors reviewed the text.

Acknowledgements

Authors would like to thank the Fundação Florestal de São Paulo, the gestors of PETAR, Intervalos and Curucutu PESHM State Parks and the Center of Zoonosis Control of the city of Itu—SP for their support in fieldwork for spider collection. Authors thank Mr. Marcos César Meneghetti for his help with animal care.

Funding

The authors also thank for the use of Cytation TM Cell Imaging Multi-Mode Reader (BioTek Instruments, Inc., Winooski, VT, USA), a Multi-User Equipment Program [Grant #15/06134-4], São Paulo Research Foundation (FAPESP). This work was supported by the following Brazilian foundations: Fundação de Amparo à Pesquisa do Estado de São Paulo (the São Paulo Research Foundation—FAPESP—Grant #15/04194-0) and Conselho Nacional de Desenvolvimento Científico e Tecnológico (the Brazilian National Council for Scientific and Technological Development—CNPq—Grant #431465/2016-9). J.M., A.P.B. and N.B. are fellows of FAPESP [#18/03051-9, #18/23559-7, #19/10003-3], and L.V. is fellow of the CNPq.

Conflict of Interest

The authors declare that the research was conducted in the absence of any commercial or financial relationships that could be construed as a potential conflict of interest.

References

- Alatrash, G., Jakher, H., Stafford, P.D., and Mittendorf, E.A. (2013) Cancer immunotherapies, their safety and toxicity. *Expert Opin. Drug Saf.* **12**, 631–645
- Thorsson, V., Gibbs, D.L., Brown, S.D., Wolf, D., Bortone, D.S., Yang, T.H.O., Porta-Pardo, E., Gao, G.F., Plaisier, C.L., Eddy, J.A., Ziv, E., Culhane, A.C., Paull, E.O., Sivakumar, I.K.A., Gentles, A.J., Malhotra, R., Farshidfar, F., Colaprico, A., Parker,

- J.S., Mose, L.E., Vo, N.S., Liu, J., Liu, Y., Rader, J., Dhankani, V., Reynolds, S.M., Bowlby, R., Califano, A., Cherniack, A.D., Anastassiou, D., Bedognetti, D., Mokrab, Y., Newman, A.M., Rao, A., Chen, K., Krasnitz, A., Hu, H., Malta, T.M., Noushmehr, H., Pedomallu, C.S., Bullman, S., Ojesina, A.I., Lamb, A., Zhou, W., Shen, H., Choueiri, T.K., Weinstein, J.N., Guinney, J., Saltz, J., Holt, R.A., Rabkin, C.S., Cancer Genome Atlas Research Network, Lazar, A.J., Serody, J.S., Demicco, E.G., Disis, M.L., Vincent, B.G., and Shmulevich, I. (2018) The immune landscape of cancer. *Immunity* **48**, 812–830
3. Burugu, S., Dancsok, A.R., and Nielsen, T.O. (2018) Emerging targets in cancer immunotherapy in *Seminars in Cancer Biology*, Vol. **52**, pp. 39–52, Academic Press, Cambridge, MA.
 4. Gotwals, P., Cameron, S., Cipolletta, D., Cremasco, V., Crystal, A., Hewes, B., Mueller, B., Quarantino, S., Sabatos-Peyton, C., Petruzelli, L., Engelman, J.A., and Dranoff, G. (2017) Prospects for combining targeted and conventional cancer therapy with immunotherapy. *Nat. Rev. Cancer* **17**, 286–301
 5. Helmy, K.Y., Patel, S.A., Nahas, G.R., and Rameshwar, P. (2013) Cancer immunotherapy: accomplishments to date and future promise. *Therap. Deliv.* **4**, 1307–1320
 6. Maus, M.V. and June, C.H. (2016) Making better chimeric antigen receptors for adoptive T-cell therapy. *Clin. Cancer Res.* **22**, 1875–1884
 7. Zhang, J. and Wang, L. (2019) The emerging world of TCR-T cell trials against cancer: a systematic review. *Technol. Cancer Res. Treat.* **18**, 15330338 19831068
 8. Looi, C.K., Chung, F.F.L., Leong, C.O., Wong, S.F., Rosli, R., and Mai, C.W. (2019) Therapeutic challenges and current immunomodulatory strategies in targeting the immunosuppressive pancreatic tumor microenvironment. *J. Exp. Clin. Cancer Res.* **38**, 162
 9. Mulder, T.A., Wahlin, B.E., Österborg, A., and Palma, M. (2019) Targeting the immune microenvironment in lymphomas of B-cell origin: from biology to clinical application. *Cancers* **11**, 915
 10. Harris, D.T., Hager, M.V., Smith, S.N., Cai, Q., Stone, J.D., Kruger, P., Lever, M., Dushek, O., Schmitt, T.M., Greenberg, P.D., and Kranz, D.M. (2018) Comparison of T cell activities mediated by human TCRs and CARs that use the same recognition domains. *J. Immunol.* **200**, 1088–1100
 11. Xu, L., Gordon, R., Farmer, R., Pattanayak, A., Binkowski, A., Huang, X., Avram, M., Krishna, S., Voll, E., Pavese, J., Chavez, J., Bruce, J., Mazar, A., Nibbs, A., Anderson, W., Li, L., Jovanovic, B., Pruell, S., Valsecchi, M., Francia, G., Betori, R., Scheidt, K., and Bergan, R. (2018) Precision therapeutic targeting of human cancer cell motility. *Nat. Commun.* **9**, 1–14
 12. Weigert, A., Mora, J., Sekar, D., Syed, S., and Brüne, B. (2016) Killing is not enough: how apoptosis hijacks tumor-associated macrophages to promote cancer progression in *Apoptosis in Cancer Pathogenesis and Anti-cancer Therapy*, pp. 205–239, Springer, Cham
 13. Komohara, Y., Fujiwara, Y., Ohnishi, K., and Takeya, M. (2016) Tumor-associated macrophages: potential therapeutic targets for anti-cancer therapy. *Adv. Drug Deliv. Rev.* **99**, 180–185
 14. Kumar, K.P., Nicholls, A.J., and Wong, C.H. (2018) Partners in crime: neutrophils and monocytes/macrophages in inflammation and disease. *Cell Tissue Res.* **371**, 551–565
 15. Alvey, C. and Discher, D.E. (2017) Engineering macrophages to eat cancer: from “marker of self” CD47 and phagocytosis to differentiation. *J. Leukocyte Biol.* **102**, 31–40
 16. DeNardo, D.G. and Ruffell, B. (2019) Macrophages as regulators of tumour immunity and immunotherapy. *Nat. Rev. Immunol.* **19**, 369–382
 17. Kowal, J., Kornete, M., and Joyce, J.A. (2019) Re-education of macrophages as a therapeutic strategy in cancer. *Immunotherapy* **11**, 677–689
 18. Cassetta, L. and Pollard, J.W. (2018) Targeting macrophages: therapeutic approaches in cancer. *Nat. Rev. Drug Discov.* **17**, 887–904
 19. Petty, A.J. and Yang, Y. (2017) Tumor-associated macrophages: implications in cancer immunotherapy. *Immunotherapy* **9**, 289–302
 20. Ruffell, B. and Coussens, L.M. (2015) Macrophages and therapeutic resistance in cancer. *Cancer Cell* **27**, 462–472
 21. Mantovani, A., Marchesi, F., Malesci, A., Laghi, L., and Allavena, P. (2017) Tumour-associated macrophages as treatment targets in oncology. *Nat. Rev. Clin. Oncol.* **14**, 399
 22. Rapôso, C., Björklund, U., Kalapothakis, E., Biber, B., da Cruz-Höfling, M.A., and Hansson, E. (2016) Neuropharmacological effects of *Phonetreria nigriventer* venom on astrocytes. *Neurochem. Int.* **96**, 13–23
 23. Barreto, D.S.N. and Bonfanti, A.P. (2019) Venom of the *Phonetreria nigriventer* spider alters the cell cycle, viability, and migration of cancer cells. *J. Cell. Physiol.* **234**, 1398
 24. Bonfanti, A.P., Barreto, N., Munhoz, J., Caballero, M., Cordeiro, G., Rocha-e-Silva, T., Sutti, R., Moura, F., Brunetto, S., Ramos, C.D., Thomé, R., Verinaud, L., and Rapôso, C. (2020) Spider venom administration impairs glioblastoma growth and modulates immune response in a non-clinical model. *Sci. Rep.* **10**, 1–16
 25. Barreto, N., Caballero, M., Bonfanti, A.P., Cezar, F., Munhoz, J., da Rocha-E-Silva, T.A.A., Sutti, R., Vitorino-Araujo, J.L., Verinaud, L., and Rapôso, C. (2020) Spider venom components decrease glioblastoma cell migration and invasion through RhoA-ROCK and Na⁺/K⁺-ATPase β 2: potential molecular entities to treat invasive brain cancer. *Cancer Cell Int.* **20**, 576
 26. Marim, F.M., Silveira, T.N., Lima, D.S. Jr., and Zamboni, D.S. (2010) A method for generation of bone marrow-derived macrophages from cryopreserved mouse bone marrow cells. *PLoS One* **5**, e15263
 27. Grippo, M.C., Penteado, P.F., Carelli, E.F., Cruz-Höfling, M.A., Verinaud, L. (2001) Establishment and partial characterization of a continuous human malignant glioma cell line: NG97. *Cell. Mol. Neurobiol.* **21**, 421–428
 28. Schenka, A.A., Machado, C.M.L., Grippo, M.C., Queiroz, L.S., Schenka, N.G.M., Chagas, C.A., Verinaud, L., Brousset, P., and Vassallo, J. (2005) Immunophenotypic and ultrastructural validation of a new human glioblastoma cell line. *Cell. Mol. Neurobiol.* **25**, 929–941
 29. Machado, C.M.L., Schenka, A., Vassallo, J., Tamashiro, W.M.S.C., Gonçalves, E.M., Genari, S.C., and Verinaud, L. (2005) Morphological characterization of a human glioma cell line. *Cancer Cell Int.* **5**, 1–7
 30. Machado, C.M.L., Ikemori, R.Y., Zorzeto, T.Q., Nogueira, A.C.M.A., Barbosa, S.D.S., Savino, W., Schenka, A.A., Vassallo, J., Heinrich, J.K., Boetcher-Luiz, F., and Verinaud, L. (2008) Characterization of cells recovered from the xenotransplanted NG97 human-derived glioma cell line subcultured in a long-term in vitro. *BMC Cancer* **8**, 291

31. Machado, C.M.L., Zorzeto, T.Q., Bianco, J.E.R., Rosa, R.G., Genari, S.C., Joazeiro, P.P., and Verinaud, L. (2009) Ultrastructural characterization of the new NG97ht human-derived glioma cell line using two different electron microscopy technical procedures. *Microsc. Res. Tech.* **72**, 310–316
32. Nicola, A.M. and Casadevall, A. (2012) In vitro measurement of phagocytosis and killing of *Cryptococcus neoformans* by macrophages in *Leucocytes*, pp. 189–197, Humana Press, Totowa, NJ
33. Naqvi, A.R., Fordham, J.B., and Nares, S. (2015) miR-24, miR-30b, and miR-142-3p regulate phagocytosis in myeloid inflammatory cells. *J. Immunol.* **194**, 1916–1927
34. Rainone, V., Martelli, C., Ottobrini, L., Biasin, M., Borelli, M., Lucignani, G., Trabattoni, D., and Clerici, M. (2016) Immunological characterization of whole tumour lysate-loaded dendritic cells for cancer immunotherapy. *PLoS One* **11**, e0146622
35. Sasaki, M., Shikata, K., Okada, S., Miyamoto, S., Nishishita, S., Usui Kataoka, H., Sato, C., Wada, J., Ogawa, D., and Makino, H. (2011) The macrophage is a key factor in renal injuries caused by glomerular hyperfiltration. *Acta Med. Okayama* **65**, 81–89
36. Pierezan, F., Mansell, J., Ambrus, A., and Hoffmann, A.R. (2014) Immunohistochemical expression of ionized calcium binding adapter molecule 1 in cutaneous histiocytic proliferative, neoplastic and inflammatory disorders of dogs and cats. *J. Comp. Pathol.* **151**, 347–351
37. Stenvinkel, P., Ketteler, M., Johnson, R.J., Lindholm, B., Pecoits-Filho, R., Riella, M., Heimbürger, O., Cederholm, T., and Girndt, M. (2005) IL-10, IL-6, and TNF- α : central factors in the altered cytokine network of uremia—the good, the bad, and the ugly. *Kidney Int.* **67**, 1216–1233
38. Ledford, H. (2011) 4 ways to fix the clinical trial: clinical trials are crumbling under modern economic and scientific pressures. Nature looks at ways they might be saved. *Nature* **477**, 526–529
39. Amaral, R.G., dos Santos, S.A., Andrade, L.N., Severino, P., and Carvalho, A.A. (2019) Natural products as treatment against cancer: a historical and current vision. *Clin. Oncol.* **4**, 1562
40. Kapellos, T.S., Taylor, L., Lee, H., Cowley, S.A., James, W.S., Iqbal, A.J., and Greaves, D.R. (2016) A novel real time imaging platform to quantify macrophage phagocytosis. *Biochem. Pharmacol.* **116**, 107–119
41. Rodell, C.B., Arlauckas, S.P., Cuccarese, M.F., Garris, C.S., Li, R., Ahmed, M.S., Kohler, R.H., Pittet, M.J., and Weissleder, R. (2018) TLR7/8-agonist-loaded nanoparticles promote the polarization of tumour-associated macrophages to enhance cancer immunotherapy. *Nat. Biomed. Eng.* **2**, 578–588
42. Kramer, N., Walzl, A., Unger, C., Rosner, M., Krupitza, G., Hengstschlager, M., and Dolznig, H. (2013) In vitro cell migration and invasion assays. *Mutat. Res. Rev. Mutat. Res.* **752**, 10–24
43. Genin, M., Clement, F., Fattaccioli, A., Raes, M., and Michiels, C. (2015) M1 and M2 macrophages derived from THP-1 cells differentially modulate the response of cancer cells to etoposide. *BMC Cancer* **15**, 1–14
44. Helm, O., Held-Feindt, J., Grage-Griebenow, E., Reiling, N., Ungefroren, H., Vogel, I., Krüger, U., Becker, T., Ebsen, M., Röcken, C., Kabelitz, D., Schäfer, H., and Sebens, S. (2014) Tumor-associated macrophages exhibit pro- and anti-inflammatory properties by which they impact on pancreatic tumorigenesis. *Int. J. Cancer* **135**, 843–861
45. Cho, U., Kim, B., Kim, S., Han, Y., and Song, Y.S. (2018) Pro-inflammatory M1 Macrophage enhances metastatic potential of ovarian cancer cells through NF- κ B activation. *Mol. Carcinogen.* **57**, 235–242
46. Chávez-Galán, L., Olleros, M.L., Vesin, D., and Garcia, I. (2015) Much more than M1 and M2 macrophages, there are also CD169+ and TCR+ macrophages. *Front. Immunol.* **6**, 263
47. Barjaktarevic, I.Z., Qadir, N., Suri, A., Santamauro, J.T., and Stover, D. (2013) Organizing pneumonia as a side effect of ipilimumab treatment of melanoma. *Chest* **143**, 858–861
48. Li, C.W., Lai, Y.J., Hsu, J.L., and Hung, M.C. (2018) Activation of phagocytosis by immune checkpoint blockade. *Front. Med.* **12**, 473–480
49. Muenst, S., Lüubli, H., Soysal, S.D., Zippelius, A., Tzankov, A., and Hoeller, S. (2016) The immune system and cancer evasion strategies: therapeutic concepts. *J. Int. Med.* **279**, 541–562
50. Genard, G., Lucas, S., and Michiels, C. (2017) Reprogramming of tumor-associated macrophages with anticancer therapies: radiotherapy versus chemo- and immunotherapies. *Front. Immunol.* **8**, 828
51. Zhou, D., Huang, C., Lin, Z., Zhan, S., Kong, L., Fang, C., and Li, J. (2014) Macrophage polarization and function with emphasis on the evolving roles of coordinated regulation of cellular signaling pathways. *Cell. Signall.* **26**, 192–197
52. Jaiswal, S., Jamieson, C.H., Pang, W.W., Park, C.Y., Chao, M.P., Majeti, R., Traver, D., van Rooijen, N., and Weissman, I.L. (2009) CD47 is upregulated on circulating hematopoietic stem cells and leukemia cells to avoid phagocytosis. *Cell* **138**, 271–285
53. Jiang, P., Lagenaur, C.F., and Narayanan, V. (1999) Integrin-associated protein is a ligand for the P84 neural adhesion molecule. *J. Biol. Chem.* **274**, 559–562
54. Zhang, M., Hutter, G., Kahn, S.A., Azad, T.D., Gholamin, S., Xu, C.Y., Liu, J., Achrol, A.S., Richard, C., Sommerkamp, P., Schoen, M.K., McCracken, M.N., Majeti, R., Weissman, I., Mitra, S.S., and Cheshier, S.H. (2016) Anti-CD47 treatment stimulates phagocytosis of glioblastoma by M1 and M2 polarized macrophages and promotes M1 polarized macrophages in vivo. *PLoS One* **11**, e0153550
55. Majeti, R., Chao, M.P., Alizadeh, A.A., Pang, W.W., Jaiswal, S., Gibbs, K.D. Jr., van Rooijen, N., and Weissman, I.L. (2009) CD47 is an adverse prognostic factor and therapeutic antibody target on human acute myeloid leukemia stem cells. *Cell* **138**, 286–299
56. Barkal, A.A., Weiskopf, K., Kao, K.S., Gordon, S.R., Rosenthal, B., Yiu, Y.Y., George, B.M., Markovic, M., Ring, N.G., Tsai, J.M., McKenna, K.M., Ho, P.Y., Cheng, R.Z., Chen, J.Y., Barkal, L.J., Ring, A.M., Weissman, I.L., and Maute, R.L. (2018) Engagement of MHC class I by the inhibitory receptor LILRB1 suppresses macrophages and is a target of cancer immunotherapy. *Nat. Immunol.* **19**, 76–84